

Electronic Supplementary Information

A Novel Strategy for Reversible Hydrogen Storage in $\text{Ca}(\text{BH}_4)_2$

Yigang Yan,^{ab} Arndt Remhof,^{*ab} Daniel Rentsch,^c Andreas Züttel,^{ad} Santanab Giri^e and Puru Jena^e

^aEMPA, Swiss Federal Laboratories for Materials Science and Technology, Materials for Energy Conversion, 8600 Dübendorf, Switzerland. Fax: +41 58 765 40 22; Tel: +41 58 765 40 82; yigang.yan@empa.ch.

^bEMPA, Swiss Federal Laboratories for Materials Science and Technology, Hydrogen & Energy, 8600 Dübendorf, Switzerland.

^cEMPA, Swiss Federal Laboratories for Materials Science and Technology, Functional Polymers, 8600 Dübendorf, Switzerland.

^dÉcole Polytechnique Fédérale de Lausanne (EPFL), Institut des Sciences et Ingénierie Chimique, Lausanne, Switzerland.

^ePhysics Department, Virginia Commonwealth University, Richmond, VA 23284, USA.

Methods

Experimental. The samples of $\text{Ca}(\text{BH}_4)_2$ (purity, 95%) and CaB_6 (purity, 95%) were purchased from Sigma-Aldrich and $\text{CaB}_{12}\text{H}_{12}$ from Katchem. The H_2 desorption of $\text{Ca}(\text{BH}_4)_2$ was performed using a custom made pressure-composition-temperature (*pct*) apparatus under dynamic vacuum (lower than 10^{-4} mbar). The samples were heated to the target temperatures with a ramp of $10^\circ\text{C}/\text{min}$. The H_2 desorption amount was recorded by a flow meter connected. After H_2 desorption, the samples were cooled rapidly to room temperature for further characterization. The rehydrogenation was carried out at 300 to 350°C under 130 to 185 bar H_2 for 80 h.

XRD measurements were performed using a Bruker D8 diffractometer equipped with a Goebel mirror selecting $\text{Cu K}\alpha$ radiation ($\lambda = 1.5418 \text{ \AA}$) and a linear detector system (Vantec). Samples for XRD measurements were filled and sealed under an argon atmosphere into glass capillaries (diameter 0.7 mm; wall thickness 0.01 mm).

Solid state ^{11}B magic angle spinning (MAS) NMR experiments were performed on a Bruker Avance-400 NMR spectrometer using a 4 mm CP-MAS probe. The ^{11}B NMR spectra were recorded at 128.38 MHz at 12 kHz sample rotation applying a Hahn echo pulse sequence to suppress the broad background resonance of boron nitride in the probe. Pulse lengths of $1.5 \mu\text{s}$ ($\pi/12$ pulse) and $3.0 \mu\text{s}$ were applied for the excitation and echo pulses, respectively. For selected samples, ^{11}B cross polarization magic angle spinning (CP-MAS) NMR experiments were performed using weak radio-frequency powers for spin locking of the ^{11}B nucleus on resonance. Solution-state NMR experiments were carried out using a 5 mm inverse broadband probe at 25°C . ^{11}B NMR chemical shifts are reported in parts per million (ppm) externally referenced to a $1\text{M B}(\text{OH})_3$ aqueous solution at 19.6 ppm as external standard sample.

Fourier transform infrared spectroscopy (FT-IR) measurements were carried out at room temperature under protective Ar atmosphere using a Bruker Alpha spectrometer equipped with a platinum ATR single reflection diamond ATR module. The calculation of IR spectrum was generated from GaussView 05 after calculating the vibrational frequency and IR intensities during optimization process.¹

Theoretical calculations. First principles calculations were carried out using density functional theory (DFT) with B3LYP hybrid functional for exchange-correlation potential.^{2,3} All calculations were performed using Gaussian 09 code with 6-311+G(d) basis sets.⁴ Since the bonding in $\text{Ca}(\text{BH}_4)_2$ is primarily covalent between B and H atoms and ionic between Ca^{2+} and $(\text{BH}_4)^-$ ions, we used a cluster approach to study the relative stability of various moieties that can form during the dehydrogenation process. Past studies have shown that this is a valid approach.⁵

We calculated the structures of BH_4^- , B_2H_6^q ($q=0, -1, -2$), B_3H_8^- , and $\text{B}_{12}\text{H}_{12}^{2-}$ moieties as well their corresponding salts, namely $\text{Ca}(\text{BH}_4)_2$, $\text{Ca}(\text{B}_2\text{H}_6)$, $\text{Ca}(\text{B}_3\text{H}_8)_2$, and $\text{Ca}(\text{B}_{12}\text{H}_{12})$. The geometries of the above clusters were optimized without any symmetry constraint. The forces and total energies were converged to 1×10^{-2} eV/Å and 1×10^{-6} eV, respectively.

Figure S1

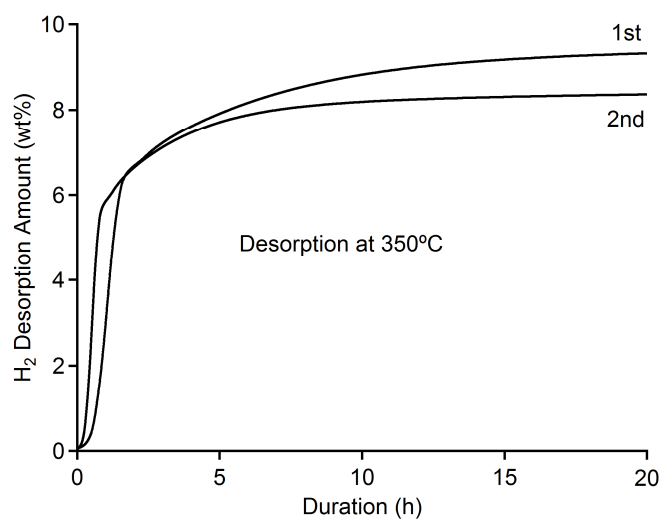


Fig. S1 Temperature-programmed-desorption (TPD) profiles of $\text{Ca}(\text{BH}_4)_2$ in the first two cycles. Desorption: 350°C, vacuum, 20h; resorption: 350°C, 185 bar H_2 , 80h

Figure S2

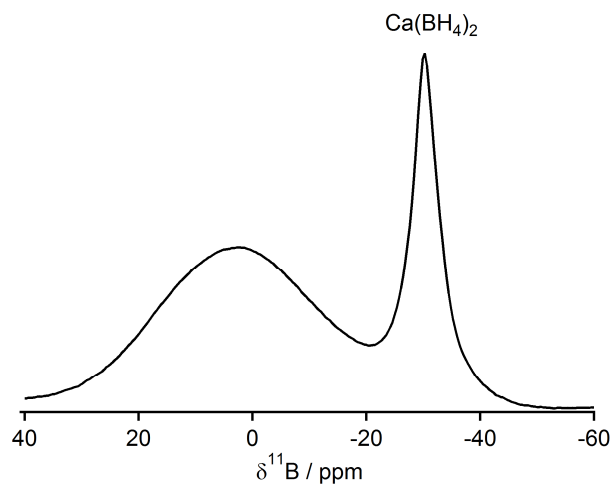


Fig. S2 ^{11}B MAS NMR spectra of rehydrogenated $\text{Ca}(\text{BH}_4)_2$ at 350°C under 185 bar H_2 . Before rehydrogenation, $\text{Ca}(\text{BH}_4)_2$ was fully dehydrogenated at 450°C for 0.5 h. A small amount of boron atom (approximately 33 %) was converted back to $\text{Ca}(\text{BH}_4)_2$.

Figure S3

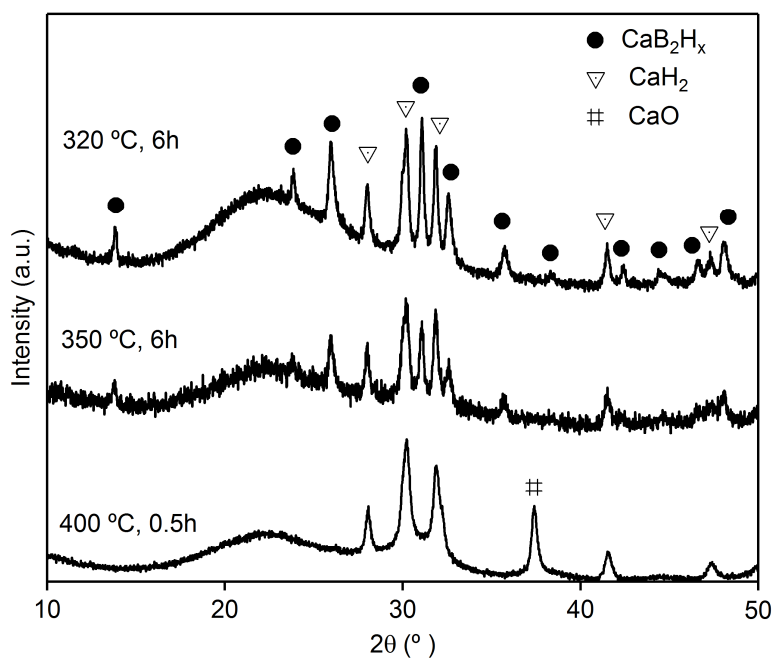


Figure S3. XRD patterns of $\text{Ca}(\text{BH}_4)_2$ after decomposition under vacuum at 320°C (6 h), 350°C (6 h) and at 400 °C (0.5 h), respectively.

Figure S4

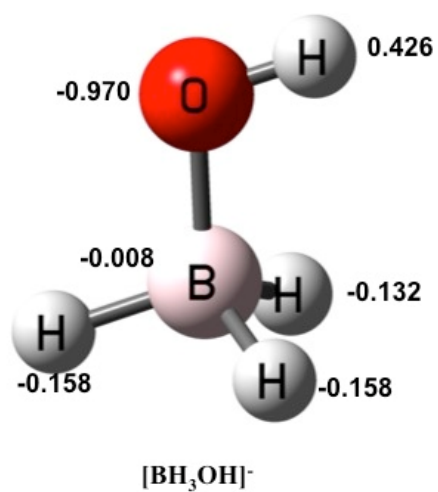


Figure S4. Optimized Geometries of $[\text{BH}_3\cdot\text{OH}]^-$ with NBO charges. The coordinates are shown in Table S1.

Table S1

Table S1. Optimized cartesian coordinates of $[\text{BH}_3\cdot\text{OH}]^-$.

Center Number	Atomic Number	Coordinates (Angstroms)		
		X	Y	Z
1	5	-0.743092	0.013874	0.000046
2	1	-1.150902	0.628925	-1.008664
3	1	-1.150576	0.630559	1.007799
4	1	-1.231547	-1.118939	0.000767
5	8	0.764162	-0.121675	0.000021
6	1	1.135187	0.763481	-0.000298

Figure S5

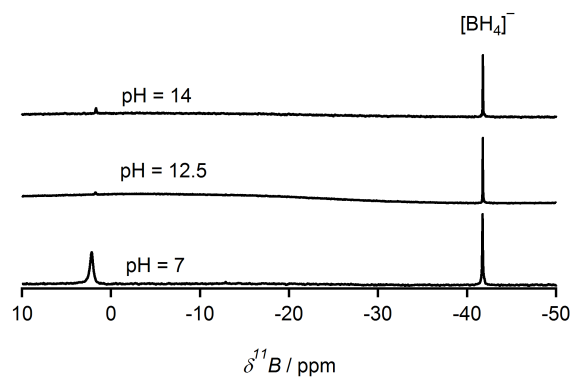


Figure S5. ^{11}B NMR spectra recorded in D_2O of $\text{Ca}(\text{BH}_4)_2$ hydrolyzed in aqueous solutions with pH value from 7 to 14.

Figure S6

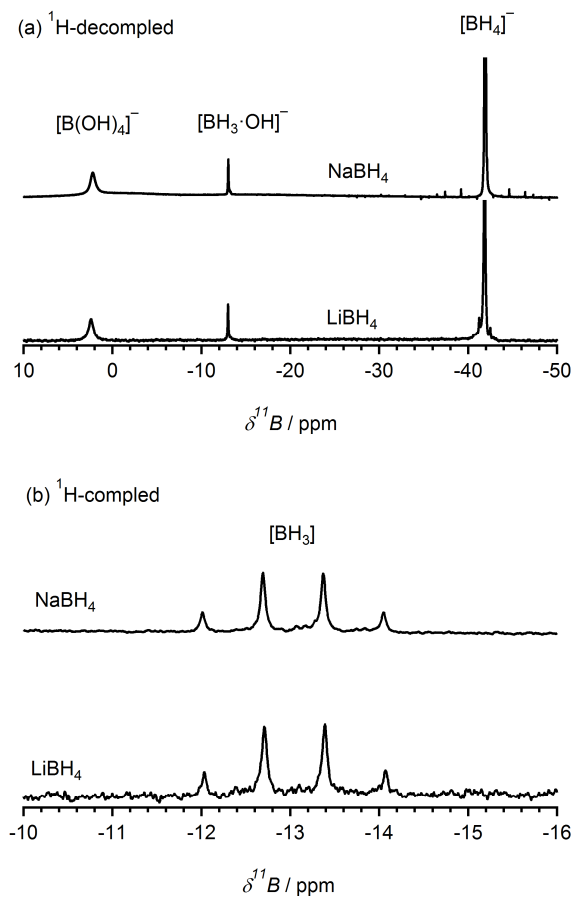


Figure S6. Hydrolysis products of NaBH_4 and LiBH_4 in D_2O observed by ^{11}B NMR spectra: (a) ^1H -coupled, (b) ^1H -decoupled. The $[\text{BH}_3]$ species show the typical quartet splitting with a ^1H , ^{11}B coupling constant of 87 Hz.

Figure S7

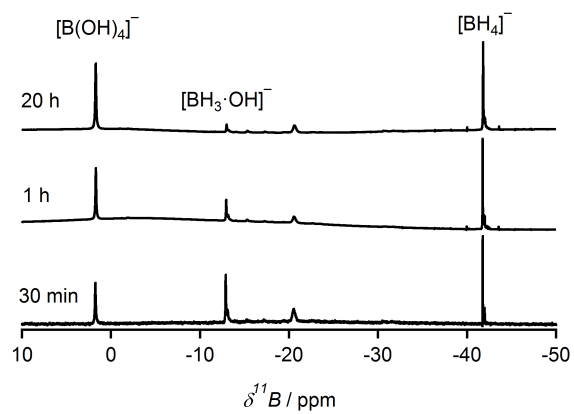


Figure S7. Decay of $[\text{BH}_3\cdot\text{OH}]^-$ observed in partially decomposed $\text{Ca}(\text{BH}_4)_2$ (350 °C, vacuum, 6 h) in alkaline solution (pH = 14, at room temperature), monitored by ^{11}B NMR spectroscopy.

Figure S8

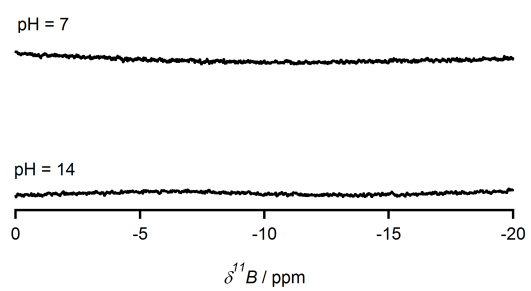


Figure S8. ^{11}B NMR spectra of CaB_6 hydrolyzed in aqueous solutions with pH value from 7 to 14.

First principles cluster calculations

First principles calculations were carried out using density functional theory (DFT) with B3LYP hybrid functional for exchange-correlation potential.^{2,3} All calculations were performed using Gaussian 09 code with 6-311+G(d) basis sets.⁴ Since the bonding in $\text{Ca}(\text{BH}_4)_2$ is primarily covalent between B and H atoms and ionic between Ca^{2+} and $(\text{BH}_4)^-$ ions, we used a cluster approach to study the relative stability of various moieties that can form during the dehydrogenation process. Past studies have shown that this is a valid approach.⁵

We calculated the structures of BH_4^- , B_2H_6^q ($q=0, -1, -2$), B_3H_8^- , and $\text{B}_{12}\text{H}_{12}^{2-}$ moieties as well their corresponding salts, namely $\text{Ca}(\text{BH}_4)_2$, $\text{Ca}(\text{B}_2\text{H}_6)$, $\text{Ca}(\text{B}_3\text{H}_8)_2$, and $\text{Ca}(\text{B}_{12}\text{H}_{12})$. The structural details were shown in Table S4. All calculations were performed using Gaussian 09 code with 6-311+G(d) basis sets. The geometries of the above clusters were optimized without any symmetry constraint. The forces and total energies were converged to 1×10^{-2} eV/Å and 1×10^{-6} eV, respectively.

We begin with the results on B_2H_6^q ($q=0, -1, -2$) moieties. The geometries of these clusters as well as Natural Bond Orbital (NBO) charges on the atoms and some representative interatomic distances are given in Fig. S9. The neutral B_2H_6 is composed of four radially bonded hydrogen atoms each carrying a charge of $-0.001e$ while each of the bridge bonded H atoms carry a charge of $+0.10e$. Each of the B atoms carries a charge of $-0.10e$. As an electron is attached the bridge bonded hydrogen atoms become radially bonded and the bond between the B atoms become weaker as seen by an increase in the B-B bond from 1.77 \AA in neutral B_2H_6 to 2.14 \AA in B_2H_6^- . The anion is only 0.13 eV lower in energy than its neutral. This is consistent with the fact that BH_3 is a stable molecule with closed electronic shells. $\text{B}_2\text{H}_6^{2-}$ dianion is metastable lying 3.69 eV above the neutral state and can only be stabilized with the help of a counter cation, in this case Ca^{2+} . The extra electron(s) in B_2H_6^- ($\text{B}_2\text{H}_6^{2-}$) is shared between the B and H atoms. BH_4^- has a perfect tetrahedral symmetry with each hydrogen atom carrying a charge of $-0.08e$ and the majority of the extra electron being located on the B atom. B_3H_8^- is composed of a triangular B network with each B atom bound to two radially bonded H atoms. Two more H atoms are bridge bonded. As in neutral B_2H_6 , the radially bonded H atoms in B_3H_8^- carry a negative charge (ranging between $-0.02e$ and $-0.03e$) while each of the bridge bonded H atoms carries a charge of $+0.11e$. In $\text{B}_{12}\text{H}_{12}^{2-}$ the B atoms remain negatively charged while the H atoms are positively charged each carrying a small charge of $+0.007e$.

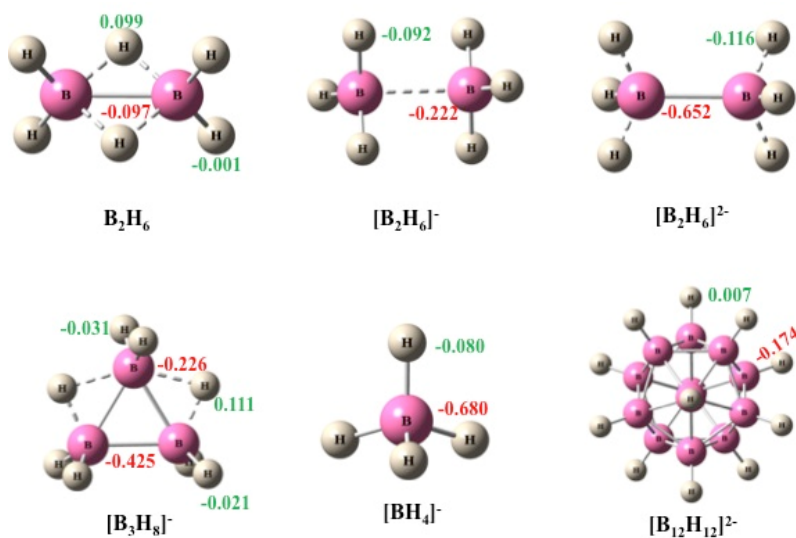


Figure S9. Optimized Geometries of Different Boranes with Representative Bond Distances (Å) and NBO charges (Red: Boron; Green: Hydrogen)

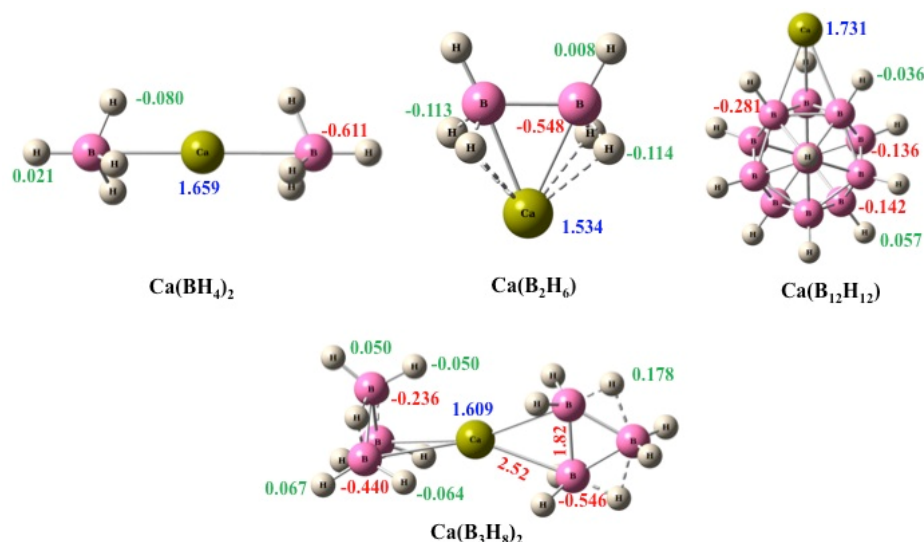


Figure S10. Optimized Geometries of Different Ca- Borane Complexes with Representative Bond Distances (Å) and NBO Charges (Red: Boron; Blue: Calcium; Green: Hydrogen)

In Fig. S10 we plot the geometries of the Ca salts made of the above anionic components. In the gas phase $\text{Ca}(\text{BH}_4)_2$ cluster forms a linear chain with the Ca^{2+} being inserted between two BH_4^- units. Here, there are two kinds of H atoms, one type carrying a charge of -0.08 while the other charged positively with a charge of +0.21e. As we will see later the two H atoms, one charged positively and the charged negatively, combine and desorb as H_2 , leaving behind $\text{Ca}(\text{B}_2\text{H}_6)$. In $\text{Ca}(\text{B}_2\text{H}_6)$ four of the H atoms carry a charge of -0.11e each while the other two carry a charge of +0.008e. The Ca atom in $\text{Ca}(\text{B}_{12}\text{H}_{12})$ is bonded to two B and one H atoms and the $\text{B}_{12}\text{H}_{12}$ unit retains the same structure as the isolated $\text{B}_{12}\text{H}_{12}^{2-}$. Structure of $\text{Ca}(\text{B}_3\text{H}_8)_2$ also exhibit similar structure where the B_3H_8 units retain the isolated geometry of B_3H_8^- discussed in the above. There are two kinds of H atoms, one carrying a positive charge while another carrying a negative charge. It is important to note that in CaB_xH_y salts, there are two different types of H atoms, one being positive while the other being negative. As in $\text{Ca}(\text{BH}_4)_2$, it is expected that in all other Ca salts the two oppositely charged H atom will combine to and desorb as a H_2 molecule.

We now discuss the relative stability of the various salts to predict the preferred intermediate phase during dehydrogenation. To accomplish this we list the total energies in Hartree atomic units of different Ca-Borane complexes and all possible products given in Table S2. Two quantities are of interest, the binding energy (Table S2), E_b and the dissociation energy, ΔE (Table S3). The binding energy of different Ca salts are defined as,

$$\begin{aligned} E_b(1) &= E(\text{Ca}^{2+}) + 2E(\text{BH}_4^-) - E[\text{Ca}(\text{BH}_4)_2] \\ E_b(2) &= E(\text{Ca}^{2+}) + E(\text{B}_2\text{H}_6^{2-}) - E[\text{CaB}_2\text{H}_6] \\ E_b(3) &= E(\text{Ca}^{2+}) + 2E(\text{B}_3\text{H}_8^-) - E[\text{Ca}(\text{B}_3\text{H}_8)_2] \\ E_b(4) &= E(\text{Ca}^{2+}) + E(\text{B}_{12}\text{H}_{12}^{2-}) - E[\text{CaB}_{12}\text{H}_{12}] \end{aligned}$$

We note that among all the Ca salts, CaB_2H_6 is most strongly bound salt followed by $\text{Ca}(\text{BH}_4)_2$, $\text{Ca}(\text{B}_3\text{H}_8)_2$ and $\text{Ca}(\text{B}_{12}\text{H}_{12})$. This would suggest that during dehydrogenation of $\text{Ca}(\text{BH}_4)_2$, the most preferred intermediate phase is $\text{Ca}(\text{B}_2\text{H}_6)$. One can also arrive at the same conclusion by calculating the dissociation energy, i.e. the energy needed to dissociate the parent salt, namely, $\text{Ca}(\text{BH}_4)_2$ into possible products. We note that the least energy needed to dissociate $\text{Ca}(\text{BH}_4)_2$ is 2.45 eV where the product is CaB_2H_6 and H_2 .

Table S2. Binding energy measured against decomposition into ions (E_b in eV) of different calcium salts.

Ca-B-H compounds	Binding Energy (E_b in eV)
$\text{Ca}(\text{BH}_4)_2$	19.85
CaB_2H_6	23.07
$\text{Ca}(\text{B}_3\text{H}_8)_2$	18.71
$\text{CaB}_{12}\text{H}_{12}$	18.22

Table S3. Dissociation energy (ΔE in eV) of $\text{Ca}(\text{BH}_4)_2$ to different compounds.

Dissociation Pathways	Dissociation Energy (ΔE in eV)
$\text{Ca}(\text{BH}_4)_2 \rightarrow \text{CaB}_2\text{H}_6 + \text{H}_2$	2.34
$\text{Ca}(\text{BH}_4)_2 \rightarrow [\text{Ca}(\text{B}_3\text{H}_8)_2 + 2 \text{CaH}_2 + 2\text{H}_2]/3$	2.45
$\text{Ca}(\text{BH}_4)_2 \rightarrow [\text{CaB}_{12}\text{H}_{12} + \text{CaB}_2\text{H}_6 + 5 \text{CaH}_2 + 14\text{H}_2]/7$	3.10
$\text{Ca}(\text{BH}_4)_2 \rightarrow [\text{CaB}_{12}\text{H}_{12} + 5 \text{CaH}_2 + 13\text{H}_2]/6$	3.23
$\text{Ca}(\text{BH}_4)_2 \rightarrow \text{B}_2\text{H}_6 + \text{CaH}_2$	3.69
$\text{CaB}_2\text{H}_6 + \text{H}_2 \rightarrow [\text{CaB}_6 + 2 \text{CaH}_2 + 10 \text{H}_2]/3$	4.63

Table S4. Number of imaginary frequency (NImag), Energy and optimized cartesian coordinates of different Boranes and Ca-Borane complexes.

System	NImag	Energy (au)	Coordinate (Cartesian)				
			Center Number	Atomic Number	Coordinates (Angstroms)		
					X	Y	Z
BH_4^-	0	-27.27045	1	5	0.000000	0.000000	0.000000
			2	1	0.715752	0.715752	0.715752
			3	1	-0.715752	-0.715752	0.715752
			4	1	-0.715752	0.715752	-0.715752
			5	1	0.715752	-0.715752	-0.715752
B_2H_6	0	-53.29544	1	5	0.883360	0.000025	0.000067
			2	1	1.458587	1.039216	0.000388
			3	1	1.459882	-1.038423	-0.000613
			4	5	-0.883401	0.000016	-0.000040
			5	1	-1.458884	1.039032	0.000169
			6	1	-1.459516	-1.038683	-0.000132
			7	1	0.000022	-0.001364	0.977491
			8	1	0.000118	0.000021	-0.977437
B_2H_6^-	0	-53.29049	1	5	-1.072025	0.001947	-0.001003
			2	1	-1.309140	-1.154406	-0.278679
			3	1	-1.280405	0.826173	-0.865670
			4	5	1.070331	-0.001779	0.000848
			5	1	1.277561	-0.809848	0.881242
			6	1	1.315252	1.157597	0.258389
			7	1	-1.293929	0.345128	1.139957
			8	1	1.299132	-0.365487	-1.134465
$\text{B}_2\text{H}_6^{2-}$	0	-53.15968	1	5	0.000000	0.000000	0.912542
			2	1	-0.587405	1.017916	1.395174
			3	1	1.175244	-0.000250	1.395174
			4	1	-0.587839	-1.017666	1.395174
			5	5	0.000000	0.000000	-0.912542
			6	1	0.587405	1.017916	-1.395174
			7	1	0.587839	-1.017666	-1.395174
			8	1	-1.175244	-0.000250	-1.395174
B_3H_8^-	0	-79.41069	1	5	0.920687	-0.537943	-0.000042
			2	5	-0.921645	-0.536448	0.000040
			3	5	0.000943	0.999066	0.000003
			4	1	1.446641	0.610333	-0.000042
			5	1	-1.446090	0.612369	0.000045
			6	1	-1.324024	-1.035491	-1.026289
			7	1	-1.323959	-1.035479	1.026400
			8	1	1.322449	-1.037405	-1.026395
			9	1	1.322518	-1.037430	1.026272
			10	1	0.001244	1.649866	-1.018276
			11	1	0.001299	1.649864	1.018283

			1	5	-0.317174	-1.667062	-0.087783
			2	5	-0.627051	-0.577987	-1.469450
			3	5	0.579397	0.738976	-1.416116
			4	5	1.635187	0.463616	-0.001322
			5	5	1.051450	-0.923799	-0.963658
			6	5	0.317145	1.667144	0.087788
			7	5	-1.080962	1.023242	-0.820096
			8	5	-0.579411	-0.738944	1.416031
			9	5	-1.051428	0.923732	0.963602
			10	5	0.627048	0.578011	1.469535
			11	5	1.080974	-1.023318	0.820149
			12	1	2.794528	0.792577	-0.001599
B ₁₂ H ₁₂ ²⁻	0	-305.74722	13	1	1.796641	-1.579163	-1.647315
			14	1	0.990507	1.262501	-2.420711
			15	1	-1.071228	-0.987977	-2.511980
			16	1	-1.846948	1.749136	-1.402009
			17	1	-0.541896	-2.849372	-0.150363
			18	1	-1.796635	1.579095	1.647259
			19	1	-0.990527	-1.262468	2.420635
			20	1	1.071212	0.987992	2.512063
			21	1	1.846953	-1.749205	1.402059
			22	1	0.541862	2.849446	0.150364
			23	5	-1.635171	-0.463610	0.001319
			24	1	-2.794489	-0.792566	0.001605
			1	5	2.420552	-0.002942	0.005255
			2	1	1.946286	-0.947950	-0.653432
			3	1	1.942720	1.037574	-0.486611
			4	1	1.936197	-0.099824	1.149050
			5	1	3.612988	-0.000302	0.010753
Ca(BH ₄) ₂	0	-732.17599	6	20	0.000092	0.002535	-0.004532
			7	5	-2.420820	-0.003129	0.004842
			8	1	-1.946716	0.968429	-0.614480
			9	1	-1.943727	-1.022011	-0.530414
			10	1	-1.934894	0.046563	1.151003
			11	1	-3.613352	0.002824	0.014289
			1	5	2.201580	0.928791	-0.011185
			2	5	2.282066	-0.895703	0.014249
			3	5	3.783152	0.085176	0.005182
			4	1	3.277572	1.531022	-0.016519
			5	1	3.404904	-1.403318	0.025416
			6	1	1.731992	-1.288028	1.028699
			7	1	1.739866	-1.315426	-0.993965
			8	1	1.619693	1.300888	0.992921
			9	1	1.627010	1.271620	-1.030336
			10	1	4.388902	0.125143	1.030401
			11	1	4.394760	0.096411	-1.017286
Ca(B ₃ H ₈) ₂	0	-836.41470	12	5	-2.650928	-0.365006	0.983542
			13	5	-2.679423	-0.612236	-0.822881
			14	5	-2.680532	1.033369	-0.128043
			15	1	-2.757305	0.837817	1.341753
			16	1	-2.804016	0.450194	-1.487759
			17	1	-1.632803	-1.090279	-1.251204
			18	1	-3.629232	-1.257478	-1.131439
			19	1	-1.589646	-0.715355	1.491431
			20	1	-3.588671	-0.898253	1.483476
			21	1	-1.621080	1.634378	-0.228123
			22	1	-3.619102	1.759986	-0.212324
			23	20	-0.111121	-0.095564	-0.011473
			1	5	1.184050	0.922869	0.002429
Ca(B ₂ H ₆)	0	-730.91341	2	1	2.244868	1.479725	-0.017607
			3	1	0.488402	1.329511	0.991409

			4	1	0.473869	1.327463	-0.979906
			5	5	1.181297	-0.924100	0.000849
			6	1	0.477079	-1.329112	0.985924
			7	1	0.474748	-1.326137	-0.984465
			8	1	2.238632	-1.487767	-0.004263
			9	20	-0.911217	0.000624	-0.000374
<hr/>							
			1	5	0.537591	-0.281676	-1.004502
			2	5	-0.459576	1.181080	-1.208124
			3	5	-1.093483	1.626914	0.415991
			4	5	0.537579	1.010183	0.258825
			5	5	-2.113168	0.279061	0.995139
			6	5	-2.114068	0.722896	-0.739085
			7	5	-0.460086	-1.637536	-0.418489
			8	5	-2.113120	-1.000913	-0.256392
			9	5	-1.093902	-1.173568	1.200716
			10	5	0.538486	-0.729944	0.745933
			11	1	1.539184	1.713983	0.438335
			12	1	-1.269413	2.766430	0.707345
Ca(B ₁₂ H ₁₂)	0	-983.32252	13	1	-0.180644	1.990121	-2.036092
			14	1	-3.052863	1.232124	-1.260145
			15	1	1.538960	-0.477172	-1.704343
			16	1	-3.052212	-1.706693	-0.436423
			17	1	-0.182007	-2.759275	-0.705223
			18	1	-1.270717	-1.995398	2.041919
			19	1	1.539817	-1.237705	1.265346
			20	1	-3.051828	0.475616	1.697025
			21	5	-1.093558	-0.453079	-1.616838
			22	5	-0.459952	0.455604	1.627126
			23	1	-1.270110	-0.770945	-2.749115
			24	1	-0.181229	0.768538	2.741705
			25	20	2.791467	0.000263	-0.000091

1. R. W. Kawiecki, F. Devlin, P. J. Stephens, R. D. Amos and N. C. Handy, *Chem Phys Lett*, 1988, **145**, 411-417.
2. A. D. Becke, *J Chem Phys*, 1993, **98**, 5648-5652.
3. C. T. Lee, W. T. Yang and R. G. Parr, *Phys Rev B*, 1988, **37**, 785-789.
4. M. J. Frisch, G. W. Trucks, H. B. Schlegel, G. E. Scuseria, M. A. Robb, J. R. Cheeseman, G. Scalmani, V. Barone, B. Mennucci, G. A. Petersson, H. Nakatsuji, M. Caricato, X. Li, H. P. Hratchian, A. F. Izmaylov, J. Bloino, G. Zheng, J. L. Sonnenberg, M. Hada, M. Ehara, K. Toyota, R. Fukuda, J. Hasegawa, M. Ishida, T. Nakajima, Y. Honda, O. Kitao, H. Nakai, T. Vreven, J. A. Montgomery Jr., J. E. Peralta, F. Ogliaro, M. J. Bearpark, J. Heyd, E. N. Brothers, K. N. Kudin, V. N. Staroverov, R. Kobayashi, J. Normand, K. Raghavachari, A. P. Rendell, J. C. Burant, S. S. Iyengar, J. Tomasi, M. Cossi, N. Rega, N. J. Millam, M. Klene, J. E. Knox, J. B. Cross, V. Bakken, C. Adamo, J. Jaramillo, R. Gomperts, R. E. Stratmann, O. Yazyev, A. J. Austin, R. Cammi, C. Pomelli, J. W. Ochterski, R. L. Martin, K. Morokuma, V. G. Zakrzewski, G. A. Voth, P. Salvador, J. J. Dannenberg, S. Dapprich, A. D. Daniels, Ö. Farkas, J. B. Foresman, J. V. Ortiz, J. Cioslowski and D. J. Fox, Gaussian, Inc., Wallingford, CT, USA, 2009.
5. Q. Sun, B. K. Rao, P. Jena, D. Stolcic, Y. D. Kim, G. Gantefor and A. W. Castleman, *J Chem Phys*, 2004, **121**, 9417-9422.